Published OnlineFirst December 8, 2009; DOI: 10.1158/1535-7163.MCT-09-0798

Antimitotic effect of the retinoid 4-oxo-fenretinide through inhibition of tubulin polymerization: a novel mechanism of retinoid growth–inhibitory activity

Valentina Appierto,[1] Paola Tiberio,[1] Elena Cavadini,[1] Patrizia Casalini,[1] Graziella Cappelletti,[2] and Franca Formelli[1]

[1]Department of Experimental Oncology and Molecular Medicine, Fondazione IRCCS "Istituto Nazionale dei Tumori"; and [2]Department of Biology, University of Milan, Milan, Italy

Abstract

The retinoid 4-oxo-*N*-(4-hydroxyphenyl)retinamide (4-oxo-4-HPR), a metabolite of fenretinide (4-HPR) present in plasma of 4-HPR–treated patients, is very effective in inducing growth inhibition and apoptosis in several cancer cell lines. 4-Oxo-4-HPR and 4-HPR have different mechanisms of action because 4-oxo-4-HPR, unlike 4-HPR, causes marked cell accumulation in G_2-M phase. Here, we investigated the molecular events involving 4-oxo-4-HPR–induced cell cycle perturbation in ovarian (A2780 and IGROV-1) and breast (T47D, estrogen receptor+ and BT-20, estrogen receptor-) cancer cells. 4-Oxo-4-HPR induced a delay of mitosis (with mitotic index increasing 5- to 6-fold in all cell lines) without progression beyond the anaphase, as shown by cyclin B1 expression. 4-Oxo-4-HPR induced multipolar spindle formation and phosphorylation of BUBR1, resulting in activation of the spindle checkpoint. Multipolar spindles were not due to impairment of pole-focusing process, loss of centrosome integrity, or modulation of the expression levels of molecules associated with spindle aberrations (Kif 1C, Kif 2A, Eg5, Tara, tankyrase-1, centractin, and TOGp). We show here that 4-oxo-4-HPR targets microtubules because, in treated cells, it interfered with the reassembly of cold-depolymerized spindle microtubules and decreased the polymerized tubulin fraction. In cell-free assays, 4-oxo-4-HPR inhibited tubulin polymerization (50% inhibition of microtubule assembly at 5.9 μmol/L), suggesting a direct molecular interaction with tubulin. In conclusion, by showing that 4-oxo-4-HPR causes mitotic arrest through antimicrotubule activities, we delineate a new molecular mechanism for a retinoid. [Mol Cancer Ther 2009;8(12):3360–8]

Introduction

Retinoids are natural and synthetic analogs of vitamin A that modulate important cellular processes, including proliferation, differentiation, and apoptosis (1). The biological activities of retinoids are mediated by the signaling of retinoic acid receptors and retinoid X receptors (2). However, the interactions with nuclear receptors do not explain all the growth-inhibitory and apoptotic effects displayed by retinoids (3). *N*-(4-hydroxyphenyl)retinamide or fenretinide (4-HPR) is a synthetic retinoid that has emerged as a promising candidate for cancer chemoprevention and chemotherapy. 4-HPR has shown efficacy against preneoplastic (4) and neoplastic conditions (5) and is well tolerated in most patients. In phase III breast cancer prevention trial, it has been shown to possibly reduce the occurrence of ovarian cancer (6) and to induce, in premenopausal women, a significant reduction of second breast cancer risk, which persists for at least 15 years (7, 8).

From the analysis of plasma samples of 4-HPR–treated patients, we have recently identified a new 4-HPR polar metabolite, 4-oxo-*N*-(4-hydroxyphenyl)retinamide (4-oxo-4-HPR) (9), which showed very promising biological proprieties (10). 4-Oxo-4-HPR showed significant growth-inhibitory and apoptotic activities in various cancer cells of different histotypes (i.e., ovarian, breast, and neuroblastoma cell lines), with potency exceeding 4-HPR in all of them (10). Another important feature of 4-oxo-4-HPR is that it is effective in 4-HPR–resistant cells and, when combined with 4-HPR, has a profound synergistic effect (10). Collectively, our previous findings suggested that 4-oxo-4-HPR might act as therapeutic agent per se and, when combined with 4-HPR, might improve 4-HPR antitumor activity or overcome 4-HPR resistance. Previous studies on 4-oxo-4-HPR antiproliferative activity have indicated that, similarly to 4-HPR, 4-oxo-4-HPR effects on cell growth are independent of nuclear retinoid receptors (10). 4-HPR and 4-oxo-4-HPR apoptotic cascades also share several signaling intermediates, such as reactive oxygen species generation, increase of ceramide production, and activation of caspase-3 and caspase-9 (10). However, despite these similarities, their mechanisms of action seem to be different because 4-oxo-4-HPR, unlike 4-HPR, causes a dramatic cell cycle arrest in G_2-M phase (10).

The present study was designed to investigate the molecular mechanisms involved in 4-oxo-4-HPR–induced cell

Received 8/26/09; accepted 10/27/09; published OnlineFirst 12/8/09.

Grant Support: The study was supported by Associazione Italiana per la Ricerca sul Cancro, Milan, Italy, through grants and a fellowship (P. Tiberio).

The costs of publication of this article were defrayed in part by the payment of page charges. This article must therefore be hereby marked *advertisement* in accordance with 18 U.S.C. Section 1734 solely to indicate this fact.

Note: Supplementary material for this article is available at Molecular Cancer Therapeutics Online (http://mct.aacrjournals.org/).

V. Appierto and P. Tiberio contributed equally to this work.

Requests for reprints: Franca Formelli, Fondazione Istituto di Ricovero e Cura a Carattere Scientifico (IRCCS) "Istituto Nazionale dei Tumori," Venezian 1, 20133 Milan, Italy. Phone: 39-02-23902706; Fax: 39-02-23902692. E-mail: franca.formelli@istitutotumori.mi.it

doi:10.1158/1535-7163.MCT-09-0798

Published OnlineFirst December 8, 2009; DOI: 10.1158/1535-7163.MCT-09-0798

cycle perturbation in breast and ovarian cancer cells. We provide evidence that 4-oxo-4-HPR induces mitotic arrest in association with multipolar spindle formation and spindle assembly checkpoint activation and show that it acts as an antimicrotubule agent by inhibiting tubulin polymerization.

Materials and Methods

Cell Lines and Reagents

Ovarian tumor cell lines A2780 (obtained from Dr. Ozols, Bethesda, MD) and IGROV-1 (obtained from Dr. Bérnard, Villejuif, France) were maintained in RPMI 1640 (Lonza) containing 10% fetal calf serum. Breast tumor cell lines T47-D and BT-20 (obtained from Dr. R. Sutherland, Sydney, New South Wales, Australia) were maintained in RPMI 1640 containing 10% fetal calf serum and 0.25 U/mL insulin. 4-Oxo-4-HPR (kindly provided by Rottapharm, Monza, IT) was dissolved at 10 mmol/L in DMSO before further dilution in culture medium and stored at −80°C in the dark. Vinblastine (Sigma) was dissolved at 1 mmol/L in water before further dilution in culture medium and stored at 4°C. In each experiment, control cells were treated with the same amount of DMSO as treated cells.

Mitotic Index

Mitotic index was determined by immunofluorescence staining with MPM-2, a monoclonal antibody with specificity for mitosis-specific phosphoproteins (11) and by DNA morphology visualized by nuclear staining with Hoechst 33342. For MPM-2 immunostaining, adherent and floating cells were collected, fixed in 4% paraformaldehyde for 10 min, and permeabilized with 100% methanol at −20°C for 7 min. Cells were then washed with PBS and spotted onto polylisinated microscope slides. After blocking in 8% bovine serum albumin (BSA)/PBS for 1 h at room temperature, cells were incubated overnight at 4°C with anti–phospho-Ser/Thr-MPM-2 (Upstate) antibody at 1:200 dilution in 1% BSA/PBS. Samples were washed with PBS and incubated with goat anti-mouse IgG/rhodamine conjugated antibody (Chemicon International) diluted 1:1,000 in 1% BSA/PBS for 1 h at room temperature and then counterstained with Hoechst 33342 (Sigma) 2 μg/mL in PBS for 2 min. Slides, mounted with Mowiol (Calbiochem), were examined by a fluorescence microscope DMRB (Leitz Microscope), and the number of cells positive for MPM-2 and with condensed chromosomes was counted (at least 200 cells per sample).

Immunofluorescence Analysis

Cells, grown on glass cover slips slides in 24-mm Petri dishes, were fixed in 100% methanol at −20°C for 7 min, washed with PBS, and then blocked at room temperature for 1 h in 3% BSA/0.1% (v/v) Triton X-100/PBS. Cells were incubated for 1 h at room temperature or overnight at 4°C in primary antibody, washed thrice with PBS, incubated for another hour at room temperature with secondary antibody, washed thrice with PBS, and stained with Hoechst 33342. Slides were mounted with Mowiol or ProLong (Invitrogen) and viewed with a fluorescence microscope [images were recorded with a Spot Insight digital camera (Delta Sistemi) equipped with a system of image analysis (IAS 2000, Delta Sistemi)] or analyzed by confocal microscopy (Microradiance 2000, Bio-Rad Laboratories) equipped with Ar (488 nm) and HeNe (543 nm) lasers. Confocal images (512 × 512 pixels) were obtained using the 60× oil immersion lens and analyzed using ImagePro 6.2 software. Reported images representing extended depth of field from 16 to 18 frames in stack (0.5 μm step) focus region were selected for maximum intensity. The pinhole diameter was regulated according to the value suggested by the acquisition software to obtain the maximum resolution power. The following antibodies were used: mouse anti–α-tubulin (Sigma), rabbit anti–γ-tubulin (Sigma), mouse anti-human cyclin B1 (Santa Cruz Biotech), mouse anti-TPX2 (Abcam), and mouse anti-NuMA (Calbiochem). The secondary antibodies used were anti-rabbit conjugated Alexa 594 and anti-mouse Alexa 488 (Molecular Probes).

Immunoblot Analysis

Proteins were extracted by lysing cells directly in SDS sample buffer (62.5 mmol/L Tris-HCl, pH 6.8; 2% SDS) containing 1 mmol/L phenylmethylsulfonyl fluoride, 10 μg/mL pepstatin, 12.5 μg/mL leupeptin, 2 μg/mL aprotinin, 1 mmol/L sodium orthovanadate, and 1 mmol/L sodium molybdate. Cell extracts were processed for Western immunoblotting, as described previously (12). The antibodies used for immunoblotting includes BUBR1 (BD Transduction Laboratories), TOGp (BioLegend), centractin/Arp1α (Sigma), α-tubulin, and actin (Sigma).

Semiquantitative Reverse Transcriptase-PCR Analysis

Semiquantitative reverse transcriptase-PCR analysis was done as previously described (12). The amplification was done using the following gene-specific oligonucleotide primers: Kif1C forward primer, 5′-AATTACCACATCCCACCCAA-3′; Kif1C reverse primer, 5′-GAACAGCAGGAACTGGCTTC-3′; Kif2A forward primer, 5′-GCCTTTGATGACTCAGCTCC-3′; Kif2A reverse primer, 5′-TTCCTGAAAAGTCACCACCC-3′; Eg5 forward primer, 5′-CAGCTGAAAAGGAAACAGCC-3′; Eg5 reverse primer, 5′-ATGAACAATCCACACCAGCA-3′; Tara forward primer, 5′-CCGCCTGTCAGAGGAGATAG-3′; Tara reverse primer, 5′-TGTGGCTCAGCTCCACATAG-3′; tankyrase-1 forward primer, 5′-GACAACAAGGCACCAATCCT-3′; tankyrase-1 reverse primer, 5′-AACCGCTCCCTCAACTTCTT-3′; β-actin forward primer, 5′-GAAATCGTGCGTGACATTAAG-3′; and β-actin reverse primer, 5′-CTAGAAGCATTTGCGGTGGACGATGGAGGGGCC-3′. Thirty-five cycles were used for Kif1C, Kif2A, Eg5, Tara, and tankyrase-1 amplification and 20 for β-actin. The PCR products were subjected to electrophoresis in agarose gel and visualized by UV after ethidium bromide staining.

Reassembly of Spindle Microtubules after Cold Treatment

Cultured cells were grown on glass cover slips in 24-mm Petri dishes and then incubated on ice for 1 h. After cold treatment, the cold medium was replaced with warm medium containing DMSO or 5 μmol/L 4-oxo-4-HPR and incubated as indicated at 37°C. Cells were fixed at different

Published OnlineFirst December 8, 2009; DOI: 10.1158/1535-7163.MCT-09-0798

time points (7, 15, and 30 min) with 100% methanol at –20°C for 7 min. The fixed cells were then processed for immunofluorescence with rabbit anti γ-tubulin and mouse monoclonal anti α-tubulin and stained with Hoechst 33342 to visualize the centrosomes, spindle microtubules, and DNA, respectively.

Tubulin Polymerization Assay

Cells were seeded in 24-mm Petri dishes and were exposed the next day to different concentration of 4-oxo-4-HPR and, 24 h later, processed for the tubulin polymerization assay (13). To separate cytosolic and cytoskeletal-associated proteins, cells were rinsed twice in PIPES-EGTA-$MgCl_2$ (PEM) buffer (85 mmol/L PIPES, pH 6.94; 10 mmol/L EGTA; 1 mmol/L $MgCl_2$; 2 mol//L glycerol; 1 mmol/L phenylmethylsulfonyl fluoride; 0.1 mmol/L leupeptin; 1 μmol/L pepstatin; 2 μg/mL aprotinin), lysed at room temperature for 10 min with PEM buffer supplemented with 0.1% v/v Triton X-100, and rinsed in PEM buffer. These Triton X-100–soluble fractions were then diluted 3:1 with 4× SDS-PAGE sample buffer. The insoluble material that remained attached to the dish was scraped into SDS-PAGE sample buffer containing protease inhibitors. Proteins were separated by SDS-PAGE, and tubulin distribution was analyzed by immunoblotting using anti α-tubulin antibody.

Tubulin Purification and Assembly Assay

Tubulin was purified from bovine brain purchased from a local slaughterhouse, conserved before use in ice-cold PIPES buffer (1 mol/L PIPES adjusted to pH 6.9 with KOH; 2 mmol/L EGTA; and 1 mmol/L $MgCl_2$), and used as soon as possible. Pure tubulin was obtained by two cycles of polymerization-depolymerization in a high-molarity buffer (14), and protein concentration was determined by the MicroBCA assay kit (Pierce). To assess the effect of 4-oxo-4-HPR and vinblastine on tubulin assembly *in vitro*, tubulin (30 μmol/L) was mixed with the compounds or vehicle in an assembly buffer (80 mmol/L K-Pipes, pH 6.9; 2 mmol/L EGTA; 1 mmol/L $MgCl_2$;1 mmol/L GTP; and 10% glycerol) and incubated at 37°C. The kinetics of tubulin polymerization was followed turbidimetrically at 350 nm in an Ultraspec 300 spectrophotometer (Pharmacia Biotech) equipped with a temperature controller. Because of the fact that 4-oxo-4-HPR (absorption maximum in methanol, 371 nm; extinction coefficient, 63.210; ref. 9) could absorb at 350 nm and consequently interfere with the increase in absorbance resulting from the polymerization of tubulin, we further evaluated microtubule assembly through a sedimentation assay. Sedimentation assay was done as previously described (15). Briefly, tubulin was mixed with the compounds and incubated in assembly buffer for 30 min at 37°C. At the end of polymerization, unpolymerized and polymerized fractions of tubulin were separated by centrifugation at 16,500 × *g* for 30 min at 30°C. The collected microtubules were resuspended in SDS-PAGE sample buffer (2% w/v SDS, 10% v/v glycerol, 5% v/v β-mercaptoethanol, 0.001% w/v bromophenol blue, and 62.5 mmol/L Tris, pH 6.8), and the unpolymerized tubulin was diluted 3:1 with 4× SDS-PAGE sample buffer. Equal proportions of each fraction were resolved by a 7.5% SDS gel and stained with Coomassie blue. Densitometric analyses of stained gels were done using the ImageMaster VDS Software (Pharmacia Biotech), and the obtained data were elaborated using SigmaPlot 8.0 program (Systat Software, Inc.). The statistical significance of 4-oxo-4-HPR effects was assessed by one-way ANOVA with Dunnet post hoc testing. All experiments were repeated at least thrice, and data were expressed as means ± SE.

Results

4-Oxo-4-HPR Causes Accumulation of Mitotic Cells in Ovarian and Breast Cancer Cell Lines

The aim of this study was to investigate the mechanism of action of 4-oxo-4-HPR, a polar metabolite of the retinoid 4-HPR, which was very effective in inducing growth inhibition and apoptosis in a large number of cancer cell lines, including ovarian and breast cancer cells. Based on flow cytometric data, we have reported that 4-oxo-4-HPR, unlike the parent drug, caused accumulation of cells in G_2-M phase in all tested cancer cell lines (10). To gain insight into mechanisms of 4-oxo-4-HPR–induced cell cycle perturbation, we analyzed whether this retinoid induced a delay of mitosis in ovarian (A2780 and IGROV-1) and breast [T47D, estrogen receptor (ER)+ and BT-20, ER-] cancer cell lines treated for 24 hours with 5 μmol/L 4-oxo-4-HPR, a dose known to effectively causes G_2-M arrest (10). The percentage of mitotic cells was analyzed by cellular staining for phospho–MPM-2 antibody, which recognizes mitosis-specific epitopes (11). The mitotic index, defined as percentage of MPM-2–positive cells, increased following 4-oxo-4-HPR treatment in all tested cancer cell lines ~5- to 6-fold (data not shown). A similar increase of mitotic index was observed by microscopic analysis of Hoechst-stained cells by scoring cells with condensed chromosomes (mitotic) in untreated and 4-oxo-4-HPR–treated cells. The nuclear staining also revealed that mitotic cells arrested by 4-oxo-4-HPR presented abnormalities in the congression of chromosomes to the metaphase plate and subsequent poleward movement. In the presence of 4-oxo-4-HPR, no mitotic figures with chromosomes aligned at the metaphase plate were found, and later mitotic configurations were not observed. An example of mitotic nuclei in T47D untreated and 4-oxo-4-HPR–treated cells is shown in Fig. 1.

Mitotic Cells Treated with 4-Oxo-4-HPR Exhibit Multipolar Spindles

Because of the incorrect organization of the condensed chromosomes in 4-oxo-4-HPR–arrested mitotic cells, we hypothesized that this retinoid could interfere with the spindle formation, and we examined the structure of mitotic spindles in A2780, IGROV-1, T47D, and BT-20 cells treated for 24 hours with 5 μmol/L 4-oxo-4-HPR. In all aforementioned cell lines, immunofluorescence labeling for α-tubulin revealed that 4-oxo-4-HPR–treated cells, in comparison with untreated cells, exhibited abnormal mitotic spindles with loss of normal bipolarity and formation of multipolar spindles (Fig. 2).

Published OnlineFirst December 8, 2009; DOI: 10.1158/1535-7163.MCT-09-0798

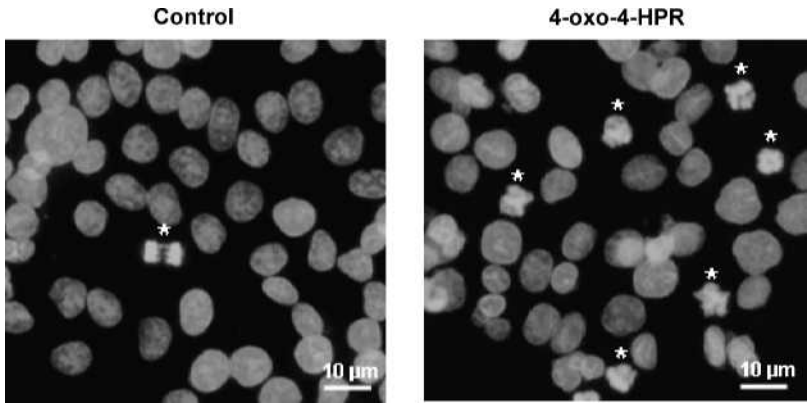

Figure 1. 4-Oxo-4-HPR induces abnormalities of chromosomes organization into metaphase plate. Nuclear morphology analysis of T47D cells treated for 24 h with DMSO or 5 μmol/L 4-oxo-4-HPR. The nuclei were stained with Hoechst 33342 and examined with a fluorescent microscope. Cells with condensed chromosomes were identified as mitotic cells (*asterisks*).

Multipolar Spindle Formation Is Not Due to Multiple Centrosomes

To further analyze the structure of the extra spindle poles, we did confocal microscopic analysis by immunofluorescence staining for spindle-pole proteins TPX2 (16) and NuMa (17) and for the centrosome component γ-tubulin (18). Because multipolar spindles seemed a common feature shared by all the four cancer cell lines, we did this and subsequent analyses only in T47D cells. In untreated cell cultures, cells in mitosis exhibited spindles (visualized by α-tubulin staining) with both poles positive for these proteins (Fig. 3). In 4-oxo-4-HPR–treated cell cultures, all poles of the multipolar spindles stained positive for TPX2 and NuMa, required for pole focusing. However, only two spots of γ-tubulin were observed. These results suggested that pole focusing was not impaired by 4-oxo-4-HPR because NuMa and TPX2 localized properly to all poles and that extranumerary poles were not induced by amplification or fragmentation of the centrosomes.

Mitotic Arrest by 4-Oxo-4-HPR Occurs in Preanaphase and Is Associated to the Spindle Checkpoint Activation

Defects of the spindle assembly typically cause mitotic arrest in preanaphase by activating the spindle mitotic checkpoint (19). We analyzed whether 4-oxo-4-HPR–induced mitotic arrest occurred in preanaphase by evaluating the expression of cyclin B1, a protein that is rapidly degraded at the metaphase-anaphase transition (20). Cells were costained with antibodies against cyclin-B1 and α-tubulin and

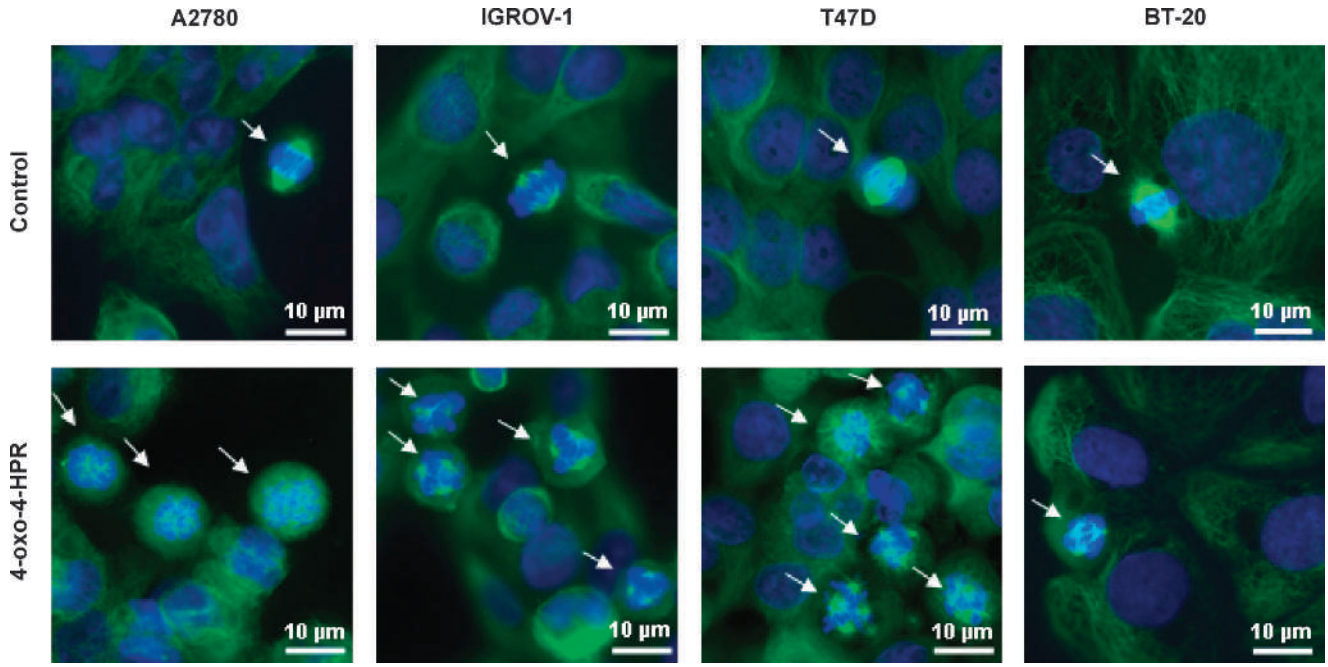

Figure 2. 4-Oxo-4-HPR induces multipolar spindle formation. Immunostaining of A2780, IGROV-1, T47D, and BT-20 cells treated with DMSO or 5 μmol/L 4-oxo-4-HPR for 24 h with α-tubulin antibody (*green*). Nuclear morphology was visualized by staining with Hoechst 33342 (*blue*). The *arrows* indicate mitotic cells.

Published OnlineFirst December 8, 2009; DOI: 10.1158/1535-7163.MCT-09-0798

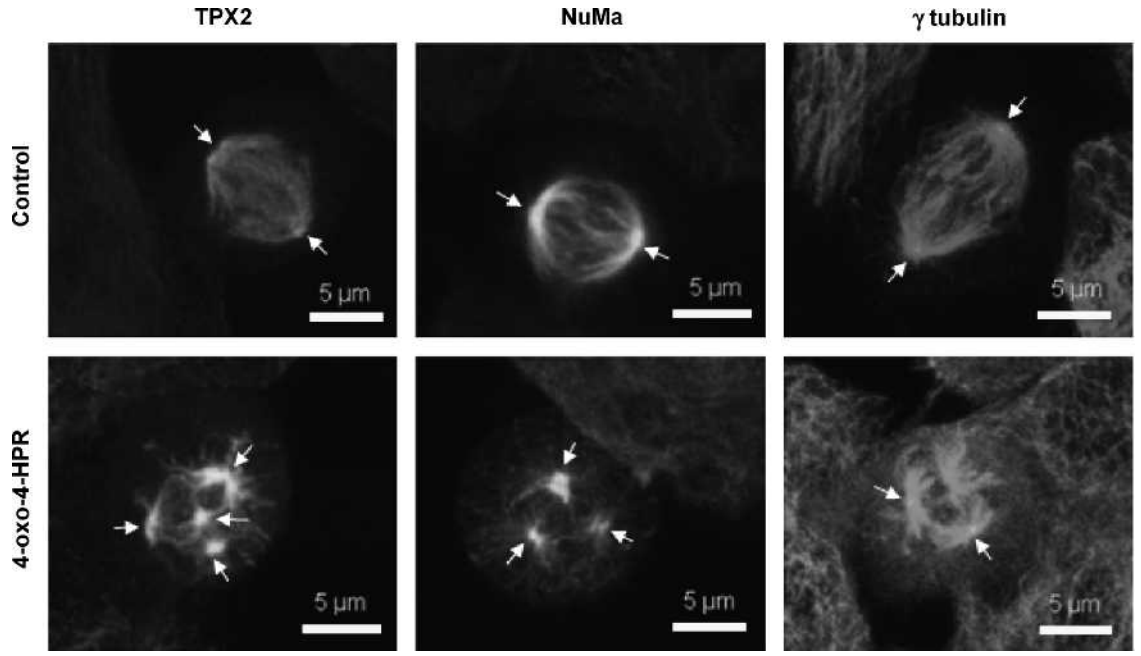

Figure 3. Multipolar spindles are not due to pole-focusing impairment or to multiple centrosomes. Representative images of confocal analysis of T47D cells treated with DMSO or 5 μmol/L 4-oxo-4-HPR for 24 h. Cells were coimmunostained with α-tubulin antibody and TPX2/NuMa/γ-tubulin. *Arrows,* TPX2, NuMa, and γ-tubulin staining.

with Hoechst 33342 to visualize DNA and score mitotic cells. As expected, mitotic cells in the absence of 4-oxo-4-HPR stained positive for cyclin B1 only before anaphase (Fig. 4A). Instead, in 4-oxo-4-HPR–treated cells, positive staining for cyclin B1 was found in almost all mitotic cells, suggesting that mitotic arrest occurred in preanaphase (Fig. 4A). To monitor whether 4-oxo-4-HPR activated the spindle checkpoint, we analyzed the phosphorylation status of BUBR1, a 120-kDa protein commonly hyperphosphorylated during this process (21). 4-Oxo-4-HPR induced phosphorylation of BUBR1, revealed as a mobility band shift in SDS-PAGE, indicating that the spindle assembly checkpoint was activated (Fig. 4B).

4-Oxo-4-HPR Does Not Affect the Expression Levels of Molecules Associated with Spindle Aberrations

To identify potential targets of 4-oxo-4-HPR, we analyzed the effect of the retinoid on the expression levels of mRNA or proteins that were overexpressed or knocked

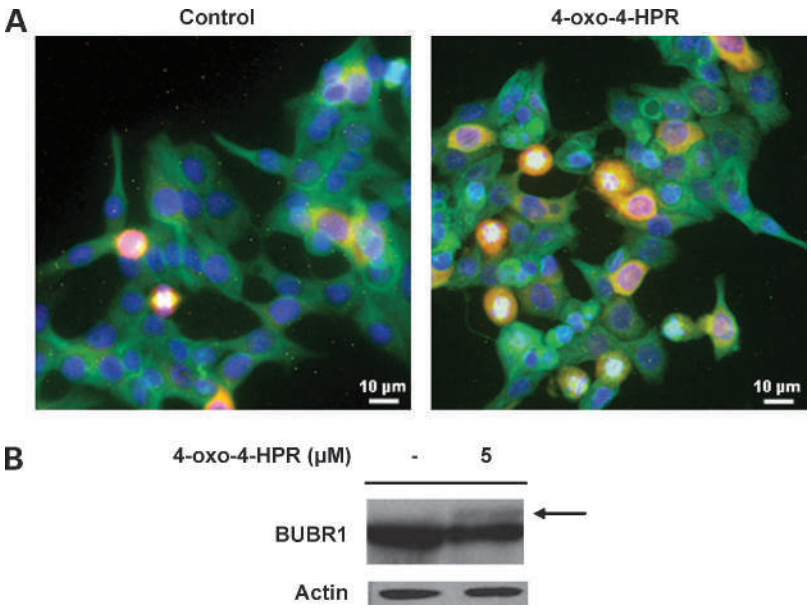

Figure 4. 4-Oxo-4-HPR induces growth arrest in preanaphase and the spindle checkpoint activation. **A,** immunostaining of T47D cells treated with DMSO or 5 μmol/L 4-oxo-4-HPR for 24 h, with cyclin B1 (*red*) and α-tubulin (*green*) antibodies. Nuclear morphology was visualized by staining with Hoechst 33342 (*blue*). **B,** Western blot analysis of phosphorylation status of BUBR1 in cells treated as in **A**. *Arrow,* BUBR1 shift. As a control for loading, the blot was incubated with actin antibody.

Published OnlineFirst December 8, 2009; DOI: 10.1158/1535-7163.MCT-09-0798

down in cells with spindle aberrations. We analyzed the mRNA expression of Kif 1C, Kif 2A, Eg5 (all members of the kinesin family proteins; ref. 22), Tara (23) and tankyrase-1 (both implicated in spindle assembly; ref. 24), and the levels of centractin (actin-related protein required for spindle orientation; ref. 25) and TOGp (a cytoskeleton-associated protein; ref. 26). None of these molecules were modulated after treatment with 5 μmol/L 4-oxo-4-HPR for 24 hours (Supplementary Figure S1), indicating that they were not likely involved in the 4-oxo-4-HPR–induced extra spindle poles formation.

4-Oxo-4-HPR Interferes with the Reassembly of Spindle Microtubules

We investigated whether 4-oxo-4-HPR interferes with mitotic spindle reassembly. To this aim, T47D cells were incubated on ice for 1 hour to depolymerize microtubules (time 0), and their reassembly was monitored 7, 15, and 30 minutes later, after incubating the cells with warm media with or without 5 μmol/L 4-oxo-4-HPR at 37°C. As shown in Fig. 5, after the cold treatment, mitotic cells in metaphase displayed a complete disassembly of spindle microtubules with centrosomes near the spindle equator and chromosomes aligned at the metaphase plate. In the absence of 4-oxo-4-HPR, normal bipolar and elongated spindles reappeared within 7 minutes upon cell rewarming, and anaphase and telophase figures were observed within 30 minutes (Fig. 5). In the presence of 4-oxo-4-HPR, the reassembly of mitotic spindles occurred as rapidly as in control mitotic cells (Fig. 5). However, spindle microtubules seemed shorter and sparser than those of the control cells, centrosomes were located near condensed chromosomes, and these morphologic characteristics persisted for up to 15 minutes. Within 30 minutes following 4-oxo-4-HPR treatment, cells exhibited mutipolar spindles, and no anaphase or telophase figures were observed (Fig. 5). These results indicated that 4-oxo-4-HPR perturbed the spindle reassembly and suggested a putative effect of the retinoid on tubulin polymerization process.

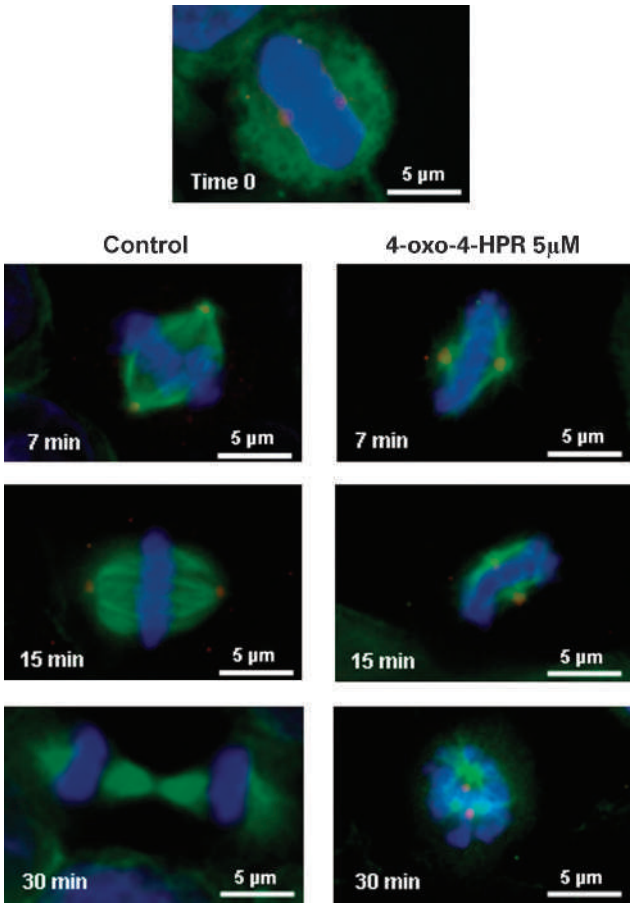

Figure 5. 4-Oxo-4-HPR interferes with the reassembly of spindle microtubules. Cultured T47D cells were incubated on ice for 1 h to depolymerize microtubules (time 0), then treated with warm medium containing DMSO or 5 μmol/L 4-oxo-4-HPR and incubated at 37°C. Cells were then fixed at different time points (7, 15, 30 min) and coimmunostained with γ-tubulin (*red*), α-tubulin (*green*), and Hoechst 33342 (*blue*) to visualize centrosomes, spindle microtubules, and DNA, respectively. A representative cell image for each time point is shown.

4-Oxo-4-HPR Inhibits Microtubule Polymerization in Cultured Cells and *In vitro*

The latter observations led us to examine whether 4-oxo-4-HPR might function as an antimicrotubule agent. Therefore, we investigated the effects of 4-oxo-4-HPR on the microtubule system of T47D cells treated for 24 hours with 4-oxo-4-HPR concentrations ranging from 3 to 10 μmol/L. Western blot analysis of free and polymerized tubulin showed that 4-oxo-4-HPR decreased the polymerized fraction of tubulin in a dose-dependent manner (Fig. 6A). This effect was confirmed in cell-free tubulin polymerization assays. 4-Oxo-4-HPR markedly interfered with the assembly kinetics of purified tubulin by lowering the initial rate and the steady-state level of polymerization, which is proportionally related to the mass concentration of the tubulin polymer (Fig. 6B). The ability of 4-oxo-4-HPR to inhibit polymerization of pure tubulin into microtubules was further investigated by sedimentation assay. Tubulin was polymerized in the absence or presence of increasing concentrations of 4-oxo-4-HPR, and assembled microtubules were separated from unpolymerized tubulin and quantified (Fig. 6C). These experiments confirmed that 4-oxo-4-HPR inhibited microtubule assembly and indicated that this effect occurs in a dose-dependent manner. The inhibition of microtubule assembly was analyzed as a function of 4-oxo-4-HPR concentration (Fig. 6D), and the value for 50% inhibition of microtubule assembly (±SEM) was 5.9 ± 1.7 μmol/L.

Discussion

From the analysis of blood samples of patients treated with the synthetic retinoid 4-HPR, we have recently identified 4-oxo-4-HPR, a novel 4-HPR polar metabolite (9). Previous *in vitro* studies conducted with this retinoid have revealed that 4-oxo-4-HPR is endowed with very promising biological proprieties and have suggested that it might be proposed as a new agent for cancer therapy, supporting

Published OnlineFirst December 8, 2009; DOI: 10.1158/1535-7163.MCT-09-0798

further investigations (10). The molecular mechanism underlying the growth inhibitory and apoptotic effects of 4-oxo-4-HPR seems to be different from that of the parent drug because of the lack of cross-resistance between these two retinoids (10). Of particular interest is the fact that 4-oxo-4-HPR, unlike 4-HPR, causes a dramatic cell cycle arrest in G_2-M phase (10).

The present study was designed to investigate the molecular mechanisms underlying 4-oxo-4-HPR–induced cell cycle arrest. Our results delineated a mechanism of action that seemed very atypical compared with the other vitamin A derivatives because of the evidence that 4-oxo-4-HPR caused mitotic arrest by acting as an antimicrotubule agent.

4-Oxo-4-HPR antimitotic activity was observed in all tested cell lines, that is, in two human ovarian (A2780 and IGROV-1) and two breast cancer cell lines, one ER+ (T47D), and one ER- (BT-20). Our finding that 4-oxo-4-HPR exerted its antimitotic activity in breast cancer cells irrespectively from their ER status could have clinical implications because there is an urgent need to identify novel preventive agents effective against ER-negative breast cancer.

Microscopic analysis of nuclear morphology in 4-oxo-4-HPR–treated cultures revealed that mitotic cells did not organize the chromosomes into a correct metaphase plate and did not progress into later mitotic phases, that is, anaphase or telophase. This feature led us to hypothesize that this retinoid could interfere with the spindle formation and prompted us to analyze the spindle structure of cells arrested in mitosis. By visualizing the spindle shape using α-tubulin staining, we determined that 4-oxo-4-HPR–induced mitotic arrest was coupled with the formation of aberrant spindles, loss of normal bipolarity, and multipolar organization. Multipolar spindles might form because of impairment of activities required for focusing microtubules (27, 28). The extra spindle poles caused by 4-oxo-4-HPR were well focused and stained positive for NuMa and TPX2, with both of these proteins required for the pole-focusing process

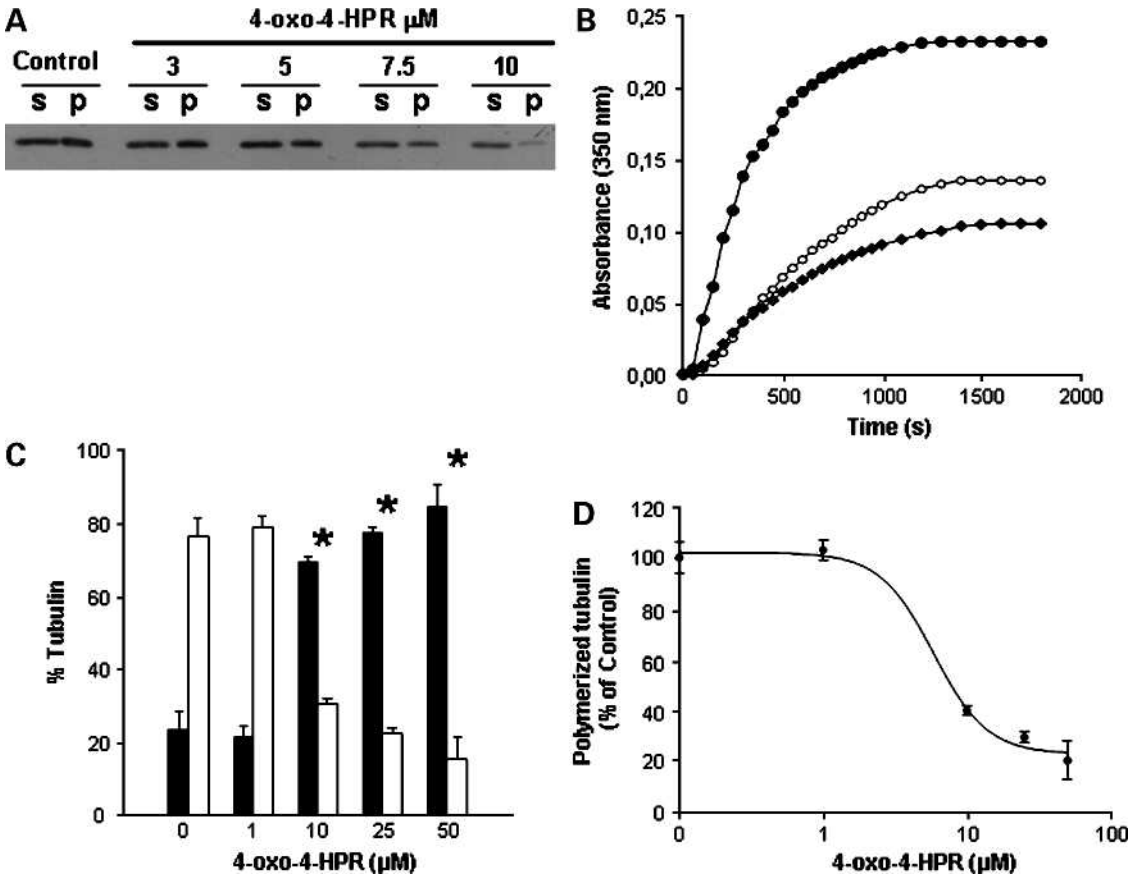

Figure 6. 4-Oxo-4-HPR inhibits tubulin polymerization in cultured cells and *in vitro*. **A,** Western blot analysis of soluble cytosolic (*s*) or polymerized (*p*) tubulin in T47D cells after 24 h of exposure to DMSO or 4-oxo-4-HPR at different doses (3, 5, 7.5, and 10 μmol/L). **B,** tubulin assembly *in vitro* was recorded as a function of time by measuring the increase in absorbance at 350 nm. Tubulin (30 μmol/L) was polymerized in assembly buffer (*filled circles*) and in the presence of 1 μmol/L vinblastine (*open circles*) or 10 μmol/L 4-oxo-4-HPR (*filled diamonds*). **C,** sedimentation assay was done in the presence or absence of increasing concentrations of 4-oxo-4-HPR; *in vitro* assembled microtubules (*white columns*) were separated by unpolymerized tubulin (*black columns*) and quantified. Values are means ± SE from three independent experiments. *, $P < 0.0005$ (one-way ANOVA with Dunnet post hoc testing). **D,** fraction of polymerized tubulin resulting from sedimentation assay is a percentage of control, plotted as a function of 4-oxo-4-HPR concentration, and fitted with a sigmoidal dose-response function. Values are means ± SE from three independent experiments.

Published OnlineFirst December 8, 2009; DOI: 10.1158/1535-7163.MCT-09-0798

(16, 17). NuMa plays an active role in organizing the microtubules at the polar region of the mitotic spindle, and its function seems to be independent from centrosomes, which are primarily responsible for microtubule nucleation (29). Similarly, TPX2 is essential for proper assembly of mitotic spindle poles and is involved in stabilizing the spindle and spindle poles (30). Pole focusing was not likely to be impaired by 4-oxo-4-HPR because NuMA and TPX2 localized properly and spindle microtubules of 4-oxo-4-HPR–arrested mitotic were focused. Another possible cause of spindle multipolarity is the presence of multiple centrosomes that can be formed by centrosome fragmentation or duplication (31, 32). It has been reported that loss of centrosome integrity in association with multipolar spindle formation can be induced by different chemical agents, including estrogens (33), combretastatin (34), rotenone (35), and arsenite (36). 4-Oxo-4-HPR–induced multipolar spindles exhibited only two centrosomes, which were visualized by γ-tubulin staining. γ-Tubulin is a member of tubulin superfamily known to be a constituent of the microtubule organizing centers (18). This observation allowed us to exclude the mechanism of multiple centrosome in the formation of aberrant spindles induced by 4-oxo-4-HPR.

Spindle assembly defects typically activate the mitotic spindle assembly checkpoint, a mechanism that monitors the proper segregation of chromosomes by preventing cell cycle progression from entering anaphase until all chromosomes have made correct attachments to the spindle (18). Our results indicated that the mitotic arrest induced by 4-oxo-4-HPR occurred before the onset of anaphase and involved activation of the spindle checkpoint because (*a*) 4-oxo-4-HPR–arrested mitotic cells were positive to cyclin B expression and degradation of cyclin B is a requisite for progression from metaphase to anaphase (20), and (*b*) 4-oxo-4-HPR caused phosphorylation of BUBR1, a protein kinase whose activity is required for checkpoint activation (21).

Altered expression levels of proteins that play key roles in maintaining bipolarity of the spindle may result in the formation of aberrant spindles. We investigated whether 4-oxo-4-HPR caused changes in the expression levels of several molecules described to have altered expression associated with monopolar or multipolar spindles. We analyzed the expression of Kif 1C, Kif 2A, and Eg5, three motor proteins belonging to the kinesin family proteins (22); Tara, implicated in cytoskeletal organization (23); tankyrase-1, a telomere-associated protein required for spindle structure (24); centractin, an actin-related protein of the dynactin complex required for spindle orientation (25); and TOGp, a microtubule-regulatory protein (26). 4-Oxo-4-HPR did not affect the expression of any of these molecules, implying that they were not involved in multipolar spindle formation induced by the retinoid.

We investigated further whether 4-oxo-4-HPR directly interfered with the spindle formation process by evaluating its effects on the reassembly of depolymerized spindle microtubules. In these experiments, cell microtubules were disassembled using cold treatment and then reversed by transferring the cells into warm medium with or without 4-oxo-4-HPR. Although, in the presence of 4-oxo-4-HPR, the spindle reassembly occurred as rapidly as in control cells, the spindle structure and function were severely impaired. Within 15 minutes, 4-oxo-4-HPR–treated cells exhibited very compressed spindles with the centrosomes still near the spindle equator, and within 30 minutes, the treatment caused mutipolar spindles formation. Contrary to the situation with control cells, no anaphase or telophase figures were observed in 4-oxo-4-HPR–treated samples. These results clearly indicated that 4-oxo-4-HPR perturbed spindle microtubule assembly dynamics. It is also noteworthy that 4-oxo-4-HPR interference in spindle reassembly occurred rapidly and that the retinoid acted in cells already in mitosis when transcription is widely repressed. These observations led us to hypothesize that 4-oxo-4-HPR might interfere with tubulin dynamics, and we tested whether it affected the microtubule polymerization process. By Western blot analysis of free and polymerized tubulin, we found that cells treated with 4-oxo-4-HPR had decreased polymerized fraction of tubulin relative to untreated cells and that this effect was dose dependent. This result was confirmed in cell-free tubulin polymerization assays, wherein 4-oxo-4-HPR showed a considerable activity in inhibiting tubulin polymerization with a 50% inhibition of microtubule assembly at 5.9 μM, a value that was substoichiometric to tubulin concentration (30 μmol/L). The follow-up *in vitro* assays also indicated a direct interaction between 4-oxo-4-HPR and tubulin whose molecular features (binding site and affinity) have not yet been investigated. Although the effect of 4-oxo-4-HPR on tubulin is proven, additional molecular mechanisms could account for its cell growth inhibitory effects. We have in fact previously shown that 4-oxo-4-HPR, similarly to 4-HPR, increases reactive oxygen species generation and ceramide levels (10). The 4-oxo-4-HPR effect on tubulin, which is different from 4-HPR, could account for its higher potency and effectiveness in 4-HPR–resistant cells.

Classic microtubule-targeted drugs, such as vinca alkaloids and taxanes, have proven to be effective for chemotherapeutic treatment of cancer (37–39). However, the clinical use of these drugs has several important limitations, including high toxicity, development of drug resistance mainly due to p-glycoprotein overexpression (40, 41), and altered expression of tubulin isotypes (42). Therefore, the characterization of new drugs targeting microtubules represents a promising research field with clinical perspectives. To our knowledge, 4-oxo-4-HPR is the first retinoid described to inhibit cell growth by targeting microtubules. Further knowledge of its resistance mechanisms, toxicity, and efficacy in combination with other drugs could reveal whether 4-oxo-4-HPR has a therapeutic potential.

In conclusion, the study on the mechanism of action of the 4-HPR metabolite 4-oxo-4-HPR uncovered a novel mechanism for retinoid growth-inhibitory activities. 4-Oxo-4-HPR causes mitotic arrest of human ovarian and breast cancer cells by inhibiting tubulin polymerization. These findings indicate that 4-oxo-4-HPR acts as an antimicrotubule agent and suggest a therapeutic potential for this retinoid for the treatment of human cancers, particularly for those that are resistant to 4-HPR and to currently used antimicrotubule drugs.

Published OnlineFirst December 8, 2009; DOI: 10.1158/1535-7163.MCT-09-0798

Disclosure of Potential Conflicts of Interest

No potential conflicts of interest were disclosed.

References

1. Nagy L, Thomazy VA, Heyman RA, Davies PJ. Retinoid-induced apoptosis in normal and neoplastic tissues. Cell Death Differ 1998; 5:11–9.

2. Mangelsdorf DJ, Thummel C, Beato M, et al. The nuclear receptor superfamily: the second decade. Cell 1995;83:835–9.

3. Altucci L, Gronemeyer H. The promise of retinoids to fight against cancer. Nat Rev Cancer 2001;1:181–93.

4. Chiesa F, Tradati N, Grigolato R, et al. Randomized trial of fenretinide (4-HPR) to prevent recurrences, new localizations and carcinomas in patients operated on for oral leukoplakia: long-term results. Int J Cancer 2005;115:625–9.

5. Garaventa A, Luksch R, Lo Piccolo MS, et al. Phase I trial and pharmacokinetics of fenretinide in children with neuroblastoma. Clin Cancer Res 2003;9:2032–9.

6. De Palo G, Mariani L, Camerini T, et al. Effect of fenretinide on ovarian carcinoma occurrence. Gynecol Oncol 2002;86:24–7.

7. Veronesi U, De Palo G, Marubini E, et al. Randomized trial of fenretinide to prevent second breast malignancy in women with early breast cancer. J Natl Cancer Inst 1999;91:1847–56.

8. Veronesi U, Mariani L, Decensi A, et al. Fifteen-year results of a randomized phase III trial of fenretinide to prevent second breast cancer. Ann Oncol 2006;17:1065–71.

9. Villani MG, Appierto V, Cavadini E, et al. Identification of the fenretinide metabolite 4-oxo-fenretinide present in human plasma and formed in human ovarian carcinoma cells through induction of cytochrome P450 26A1. Clin Cancer Res 2004;10:6265–75.

10. Villani MG, Appierto V, Cavadini E, et al. 4-Oxo-fenretinide, a recently identified fenretinide metabolite, induces marked G2/M cell cycle arrest and apoptosis in fenretinide-sensitive and -resistant cell lines. Cancer Res 2006;66:3238–47.

11. Davis FM, Tsao TY, Fowler SK, Rao PN. Monoclonal antibodies to mitotic cells. Proc Natl Acad Sci 1983;80:2926–30.

12. Appierto V, Villani MG, Cavadini E, Lotan R, Vinson C, Formelli F. Involvement of c-Fos in fenretinide-induced apoptosis in human ovarian carcinoma cells. Cell Death Differ 2004;1:270–9.

13. Cappelletti G, Tedeschi G, Maggioni MG, Negri A, Nonnis S, Maci R. The nitration of tau protein in neurone-like PC12 cells. FEBS Lett 2004; 562:35–9.

14. Castoldi M, Popov AV. Purification of brain tubulin through two cycles of polymerization-depolymerization in a high-molarity buffer. Protein Expr Purif 2003;32:83–8.

15. Passarella D, Giardini A, Peretto B, et al. Inhibitors of tubulin polymerization: synthesis and biological evaluation of hybrids of vindoline, anhydrovinblastine and vinorelbine with thiocolchicine, podophyllotoxin and baccatin III. Bioorg Med Chem 2008;16:6269–85.

16. Gruss OJ, Vernos I. The mechanism of spindle assembly: functions of Ran and its target TPX2. J Cell Biol 2004;66:949–55.

17. Sun QY, Schatten H. Role of NuMA in vertebrate cells: review of an intriguing multifunctional protein. Front Biosci 2006;11:1137–46.

18. Cuschieri L, Nguyen T, Vogel J. Control at the cell center: the role of spindle poles in cytoskeletal organization and cell cycle regulation. Cell Cycle 2007;6:2788–94.

19. Clarke PR, Allan LA. Cell-cycle control in the face of damage—a matter of life or death. Trends Cell Biol 2009;19:89–98.

20. Clute P, Pines J. Temporal and spatial control of cyclin B1 destruction in metaphase. Nat Cell Biol 1999;1:82–7.

21. Li W, Lan Z, Wu H, et al. BUBR1 phosphorylation is regulated during mitotic checkpoint activation. Cell Growth Differ 1999;10:769–75.

22. Zhu C, Zhao J, Bibikova M, et al. Functional analysis of human microtubule-based motor proteins, the kinesins and dyneins, in mitosis/cytokinesis using RNA interference. Mol Biol Cell 2005;16:3187–99.

23. Yu J, Lan J, Zhu Y, et al. The E3 ubiquitin ligase HECTD3 regulates ubiquitination and degradation of Tara. Biochem Biophys Res Commun 2008;367:805–12.

24. Chang P, Coughlin M, Mitchison TJ. Tankyrase-1 polymerization of poly(ADP-ribose) is required for spindle structure and function. Nat Cell Biol 2005;7:1133–9.

25. Clark IB, Meyer DI. Overexpression of normal and mutant Arp1α (centractin) differentially affects microtubule organization during mitosis and interphase. J Cell Sci 1999;112:3507–18.

26. Holmfeldt P, Stenmark S, Gullberg M. Differential functional interplay of TOGp/XMAP215 and the KinI kinesin MCAK during interphase and mitosis. EMBO J 2004;23:627–37.

27. Quintyne NJ, Reing JE, Hoffelder DR, Gollin SM, Saunders WS. Spindle multipolarity is prevented by centrosomal clustering. Science 2005; 307:127–9.

28. Garrett S, Auer K, Compton DA, Kapoor TM. hTPX2 is required for normal spindle morphology and centrosome integrity during vertebrate cell division. Curr Biol 2002;12:2055–9.

29. Gaglio T, Saredi A, Compton DA. NuMA is required for the organization of microtubules into aster-like mitotic arrays. J Cell Biol 1995;131: 693–708.

30. Wittmann T, Wilm M, Karsenti E, Vernos I. TPX2, A novel xenopus MAP involved in spindle pole organization. J Cell Biol 2000;149:1405–18.

31. Lingle WL, Lukasiewicz K, Salisbury JL. Deregulation of the centrosome cycle and the origin of chromosomal instability in cancer. Adv Exp Med Biol 2005;570:393–421.

32. Gisselsson D. Mitotic instability in cancer: is there method in the madness? Cell Cycle 2005;4:1007–10.

33. Ochi T, Oda T. Structure-effect relationship in the induction of mitotic phase-specific abnormality of centrosome integrity and multipolar spindles by steroidal estrogens and their derivatives in cultured mammalian cells. J Steroid Biochem Mol Biol 2001;78:113–22.

34. Cenciarelli C, Tanzarella C, Vitale I, et al. The tubulin-depolymerising agent combretastatin-4 induces ectopic aster assembly and mitotic catastrophe in lung cancer cells H460. Apoptosis 2008;13:659–69.

35. Diaz-Corrales FJ, Asanuma M, Miyazaki I, Miyoshi K, Ogawa N. Rotenone induces aggregation of γ-tubulin protein and subsequent disorganization of the centrosome: relevance to formation of inclusion bodies and neurodegeneration. Neuroscience 2005;133:117–35.

36. Yih LH, Tseng YY, Wu YC, Lee TC. Induction of centrosome amplification during arsenite-induced mitotic arrest in CGL-2 cells. Cancer Res 2006;66:2098–106.

37. van Tellingen O, Sips JH, Beijnen JH, Bult A, Nooijen WJ. Pharmacology, bio-analysis and pharmacokinetics of the vinca alkaloids and semisynthetic derivatives. Anticancer Res 1992;12:1699–715.

38. Rowinsky EK. The development and clinical utility of the taxane class of antimicrotubule chemotherapy agents. Annu Rev Med 1997; 48:353–74.

39. Crown J, O'Leary M. The taxanes: an update. Lancet 2000;355: 1176–8.

40. Gottesman MM, Pastan I. Biochemistry of multidrug resistance mediated by the multidrug transporter. Annu Rev Biochem 1993;62: 385–427.

41. Bradley G, Ling V. P-glycoprotein, multidrug resistance and tumor progression. Cancer Metastasis Rev 1994;13:223–33.

42. Burkhart CA, Kavallaris M, Band Horwitz S. The role of β-tubulin isotypes in resistance to antimitotic drugs. Biochim Biophys Acta 2001; 1471:O1–9.

AACR American Association for Cancer Research

Molecular Cancer Therapeutics

Antimitotic effect of the retinoid 4-oxo-fenretinide through inhibition of tubulin polymerization: a novel mechanism of retinoid growth–inhibitory activity

Valentina Appierto, Paola Tiberio, Elena Cavadini, et al.

Mol Cancer Ther 2009;8:3360-3368. Published OnlineFirst December 8, 2009.